Journal of Cellular and Molecular Medicine
A JOURNAL OF TRANSLATIONAL MEDICINE

J. Cell. Mol. Med. Vol 16, No 1, 2012 pp. 118-128

Embryonic liver fodrin involved in hepatic stellate cell activation and formation of regenerative nodule in liver cirrhosis

Zhijun Wang [a, b], Fang Liu [c], Wei Tu [b], Ying Chang [b], Jinjian Yao [b], Wei Wu [b], Xiang Jiang [b], Xingxing He [b], Jusheng Lin [b], Yuhu Song [a, *]

[a] *Department of Gastroenterology, Union Hospital, Tongji Medical College, Huazhong University of Science and Technology, Wuhan, China*
[b] *Institute of Liver Diseases, Tongji Hospital, Tongji Medical College, Huazhong University of Science and Technology, Wuhan, China*
[c] *Institute of Hematology, Union Hospital, Tongji Medical College, Huazhong University of Science and Technology, Wuhan, China*

Received: October 24, 2010; Accepted: January 28, 2011

Abstract

Transforming growth factor (TGF) β_1 plays a critical role in liver fibrosis. Previous studies demonstrated embryonic liver fodrin (ELF), a β-spectrin was involved in TGF-β/Smad signalling pathway as Smad3/4 adaptor. Here we investigate the role of ELF in pathogenesis of liver cirrhosis. In carbon tetrachloride (CCl_4)-induced mice model of liver cirrhosis, ELF is up-regulated in activated hepatic stellate cells (HSCs), and down-regulated in regenerative hepatocytes of cirrhotic nodules. In activated HSCs *in vitro*, reduction of ELF expression mediated by siRNA leads to the inhibition of HSC activation and procollagen I expression. BrdU assay demonstrates that down-regulation of ELF expression does not inhibit proliferation of activated HSCs *in vitro*. Immunostaining of cytokeratin 19 and Ki67 indicates that regenerative hepatocytes in cirrhotic liver are derived from hepatic progenitor cells (HPC). Further study reveals that HPC expansion occurs as an initial phase, before the reduction of ELF expression in regenerative hepatocytes. Regenerative hepatocytes in cirrhotic liver show the change in proliferative activity and expression pattern of proteins involved in G1/S transition, which suggests the deregulation of cell cycle in regenerative hepatocytes. Finally, we find that ELF participates in TGF-β/Smad signal in activated HSCs and hepatocytes through regulating the localization of Smad3/4. These data reveal that ELF is involved in HSC activation and the formation of regenerative nodules derived from HPC in cirrhotic liver.

Keywords: β_2-Spectrin • hepatic stellate cell • hepatic progenitor cell • liver cirrhosis

Introduction

Transforming growth factor (TGF-β) represents a large family of growth and differentiation factors that regulate cell differentiation, proliferation, migration, motility, adhesion and apoptosis. TGF-β signalling pathway is activated upon ligand binding to types II and I transmembrane receptor serine/threonine kinase, which subsequently phosphorylates receptor-associated Smad proteins (Smad2 and Smad3). Smad2/3 forms heteromeric complexes with Smad4. The complexes translocate to the nucleus and activate target genes [1, 2]. Adaptor proteins, such as embryonic liver fodrin (ELF), Smad anchor for receptor activation (SARA) and filamin play a critical role in modulating the activity of receptor-associated Smad and Smad4 through the control of Smad access to TGF-β receptor [3, 4]. β-Spectrins (Spn), major dynamic scaffold molecules, are involved in the maintenance of cell shape, establishment of cell polarity and protein sorting [5, 6]. ELF, a β-spectrin, has been demonstrated to play a pivotal role in TGF-β signalling [7, 8]. It is involved in TGF-β/Smad signalling pathway as an adaptor [7, 8]. ELF does not appear to interact with SARA or filamin [8].

Liver fibrosis or cirrhosis, the ultimate pathological consequence of severe chronic liver damage, represents a major medical problem with significant morbidity and mortality worldwide.

*Correspondence to: Yuhu SONG,
Department of Gastroenterology, Union Hospital, Tongji Medical College, Huazhong University of Science and Technology,
Wuhan 430022, China.
Tel.: +86-2785726381
Fax: +86-2785726086
E-mail: yuhusong@yahoo.com or yhsong@tjh.tjmu.edu.cn

doi: 10.1111/j.1582-4934.2011.01290.x

Liver cirrhosis is characterized by deposition of extracellular matrix (ECM), the distortion of the liver parenchyma replaced by regenerative nodules, altered blood flow. Upon chronic injury, quiescent hepatic stellate cells (HSCs) in space of Disse transdifferentiate into myofibroblast-like cells, acquiring contractile, proliferative and fibrogenic properties [9–11]. Of cytokines involved in liver fibrogenesis, TGF-β_1 is the most potent profibrogenic mediator [10, 12–15]. TGF-β_1 transforms HSCs into myofibroblasts, which results in up-regulation of many ECM proteins and down-regulation of their degradation by matrix metalloproteinases and tissue inhibitor of metalloproteinases. Blockade of the TGF-β signal by dominant negative type II TGF receptor suppressed the development of dimethylnitrosamine-induced hepatic fibrosis [16, 17]. Inhibition of TGF-β_1 expression mediated by siRNA and ribozyme blocked ECM deposition [18, 19]. In view of the importance of TGF-β signal in liver fibrosis, we hypothesize that ELF, an adaptor in TGF-β signalling pathway may play a key role in liver cirrhosis. Therefore, we examined ELF expression in cirrhotic liver and evaluated the role of ELF in liver cirrhosis. In this study, we demonstrate that ELF is required for HSC activation and ECM deposition in activated HSCs cultured *in vitro*; in addition, interestingly, ELF down-regulation in regenerative hepatocytes is involved in the formation of regenerative nodules derived from hepatic progenitor cells (HPC). Thus, this study has identified, for the first time, a molecule participates in liver cirrhosis through the involvement of HSC activation and the formation of regenerative nodule.

Materials and methods

Mice models of acute liver injury and liver cirrhosis

Liver cirrhosis

C57/Black/6 mice were purchased from Animal Center of Tongji Medical College, Huazhong University of Science and Technology (Wuhan, China). The mice were injected subcutaneously with carbon tetrachloride (CCl_4) diluted 3:7 (v/v) ratio in olive oil or olive oil (control) at a dose of 5 ml/kg twice a week for 12 weeks. Mice were sacrificed 48 hrs after the last injection.

Acute

Mice were injected intraperitoneally with 5 ml/kg CCl_4 diluted 3:7 (v/v) ratio in olive oil or olive oil (control). The mice were sacrificed at 20 hrs after administration. The protocol of animal treatment used in this study was approved by the institutional animal care and use committee.

Real-time RT-PCR

Total RNA isolated from culture cells and liver tissue was reverse transcribed into cDNA (Takara, DRR037S, Dalian, China), and then real time quantitative PCR was performed using Stratagene MX3000 and SYBR premix EX TAQ (Takara, DRR041S). The following primers were used: ELF (NM_009260.2) forward: 5′-GAG TTG CAG AGG ACA TCC AGC-3′, reverse: 5′-ATT-GAC CCA CTT GGT GAA GGT C-3′; α-SMA (NM_007392) forward: 5′-CGG GAG AAA ATG ACC CAG ATT-3′ reverse: 5′-GGA CAG CAC AGC CTG AAT AGC-3′; procollagen I alpha 1 (NM_007742) forward: 5′-ACG GCT GCA CGA GTC ACA- 3′ reverse: 5′-AAG GGA GCC ACA TCG ATG AT-3′; CK19 (NM_008471) forward: 5′- CCC TCC AGG GCC TTG AGA T-3′, reverse: 5′-TCT GTG ACA GCT GGA CTC CAT AA-3′; GAPDH (NM_008084) forward: 5′-ACC CAG AAG ACT GTG GAT GG-3′, reverse: 5′-ACA CAT TGG GGG TAG GAA CA-3′; the N-termini specific primers for ELF, isoform 2 Spnb 2 were designed because isoform 2 has shorter and distinct N- and C-termini compared with isoform 1.

Immunoprecipitation and Western blot

Lysates from cells and tissues were collected using RIPA buffer (Sigma R0278, St Louis, MO, USA), and then immunoprecipitated with 1 μg primary antibody. The specimens were resolved over SDS-polyacrylamide gels, incubated with primary antibody, then with peroxidase-conjugated secondary antibody. Immmunoreactive bands were visualized with ECL detection kit (Thermo 34077, Rockford, IL, USA). The following primary antibodies were used: ELF [20] (1 in 400 dilution), Smad2 (1 in 500 dilution, Proteintech lab 12570-1-AP, Chicago, IL, USA), Smad3 (1 in 400 dilution, Abcam AB28379, Cambridge, MA, USA), Smad4 (1 in 500 dilution, Santa Cruz SC-1909, Santa Cruz, CA, USA), α-SMA (1 in 500 dilution, Abcam AB5694), CDK4 (1 in 500 dilution, Proteintech lab 11026-1-AP), proliferating cell nuclear antigen (PCNA) (1 in 500 dilution, Proteintech lab 10205-1-AP), cyclinD1 (1 in 500 dilution, Proteintech lab 10438-1-AP), pRb (1 in 1000 dilution, Santa Cruz SC-7986) and GAPDH (1: 500 dilution, Proteintech lab 60004-1).

Immunohistochemistry and immunofluoresence

Paraffin-embedded sections of liver and cells grown on the cover slips were processed for immunohistochemistry and inmmunofluoresence. Immunohistochemical staining was performed by using elite ABC kit (Vector labs PK-7200, Burlingame, CA, USA). For immunofluorescence, rabbit and goat primary antibodies were visualized with Cy2- or Cy3-conjugated secondary antibodies (Jackson ImmunoResearch, West Grove, PA, USA). Antibody against ELF (1:100 dilution), Smad3 (1:100 dilution), Smad4 (1:100 dilution), α-SMA (1:100 dilution), PCNA (1:100 dilution), CK19 (Proteintech lab 10712-1-AP), Ki67 (1:100 dilution, Abcam AB15580), albumin (1:100 dilution, Proteintech lab 16475-1-AP) were applied according to the manufacturer's instruction.

HSC and hepatocyte isolation

HSC isolation

Mice HSCs were isolated from wild-type C57/Black/6 mice by *in situ* perfusion with pronase E and collagnease type I followed by differential centrifugation on Opti-Prep (Sigma) density gradients, as described previously [21]. Mouse livers were perfused *in situ* sequentially with ethylene *bis*(2-aminoethyl) glycol tetraacetic acid (EGTA) solution and the buffer containing 180 mg/l collagenase type I (Invitrogen, Carlsbad, CA, USA),

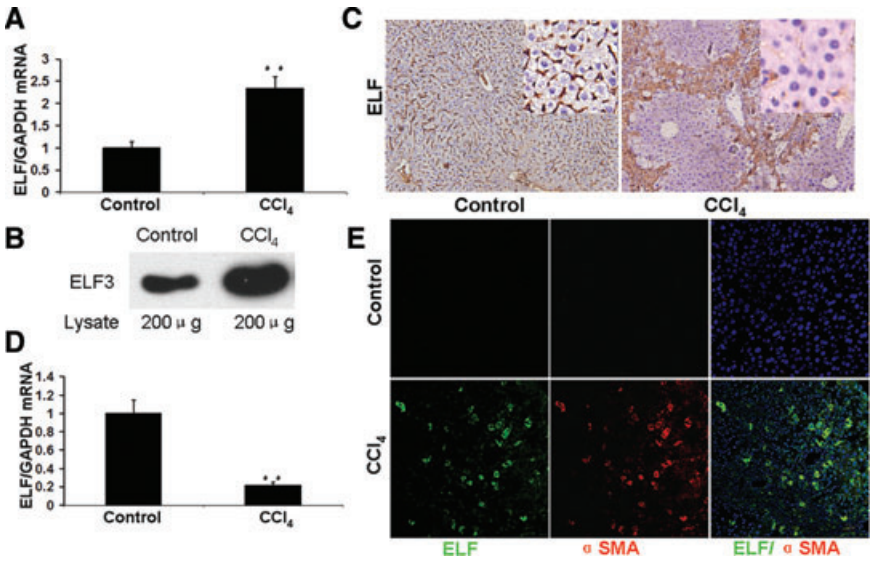

Fig. 1 ELF expression in cirrhotic liver. (**A**) Real-time RT-PCR quantification of ELF mRNA transcript in whole liver homogenates from control and chronic CCl_4 treated mice. $P < 0.01$: for chronic CCl_4-treated mice *versus* control mice. (**B**) Hepatic level of ELF protein was determined by Western blot analysis. (**C**) ELF expression in cirrhotic liver was determined by immunohistochemical analysis. Magnification, 200×. (**D**) ELF expression in hepatocytes isolated from control or chronic CCl_4-treated mice was evaluated by real-time RT-PCR. $P < 0.01$: for chronic CCl_4-treated mice *versus* control mice. (**E**) Colocalization of ELF and α-SMA in activated HSCs *in vivo*. Liver section was stained with ELF antibody (green); SMA antibody (red) and DAPI (blue). Magnification 200×.

400 mg/l pronase E (Roche, Mannheim, Germany) and 0.02% DNase I (Invitrogen). Then the excised liver was digested in the digestion solution (180 mg/l collagenase type I, 400 mg/l pronase E and 0.02% DNase I) at 37°C for 20 min with gentle stirring. The homogenate was filtered and centrifuged at 25 × *g* for 5 min to remove the hepatocytes. The supernatant was centrifuged on Opti-prep (Sigma) density gradients as described previously [21]. Cell viability assessed by trypan blue exclusion was always greater than 90%. Purity of freshly isolated HSCs identified by retinoid autofluorescence was always greater than 90%. Primary HSCs were cultured in DMEM/10% foetal bovine serum (FBS) containing penicillin and streptomycin.

Hepatocyte isolation

Primary hepatocytes were isolated by a two-step perfusion technique. Mice hepatocytes were isolated from the digested liver by centrifugation over Opti-Prep density Gradients [22, 23]. Cell viability assessed by trypan blue exclusion was more than 90%. Primary hepatocytes and AML-12 cells were cultured in DMEM/10% FBS containing penicillin and streptomycin.

Preparation and transfection of siRNAs

Chemically synthesized siRNAs directed against ELF were purchased from A&B Applied Biosystems. ELF siRNAs (50 pmol) and scrambled siRNAs (50 pmol) used as negative control were transduced into mice HSCs on six wells by using lipofectamine 2000 (Invitrogen) when HSCs reached 30–50% confluence. After 72 hrs, transfected cells were collected for further study. ELF siRNA s74307 was selected for subsequent experiment because of its greatest efficacy.

BrdU assay

Cells seed on 96-well plates were treated with test reagents, and then BrdU (Millipore 2750, Billerica, MA, USA) was incorporated into proliferating cell for 6 hrs. BrdU assay was performed according to the manufacturer's protocol. In brief, after BrdU incorporation, the cells were fixed and incubated with anti-BrdU monoclonal antibody for 1 hr. After washing with PBS, they were incubated with goat antimouse peroxidase-conjugated IgG antibody, substrate and stop solution. The amount of BrdU is determined through reading the plate using a spectrophotometer microplate reader set.

Statistical analyses

Results are expressed as mean ± S.E.M. Significance of the difference between means was analysed either by Student's t-test or by ANOVA. $P < 0.05$ was taken as the minimum level of significance.

Results

ELF expression in cirrhotic liver

To determine whether ELF was involved in hepatic cirrhosis, we evaluated ELF expression in cirrhotic liver induced by 12-week injection of CCl_4. Mice model of liver cirrhosis was confirmed by the staining of haematoxylin–eosin, sirius red staining (Fig. S1) and α smooth muscle actin (SMA) (Fig. S2). Real-time RT-PCR (Fig. 1A) and Western blot analysis (Fig. 1B) showed ELF expression increased significantly in CCl_4-treated mice compared with the control. To further investigate ELF distribution in cirrhotic liver, we performed immunohistochemical staining. Immunohistochemical results showed that ELF was found mainly at the plasma membrane, and absent in the cytoplasm in liver of control mice; ELF expression and distribution changed in cirrhotic liver. Surprisingly, ELF expression increased mainly in the areas of

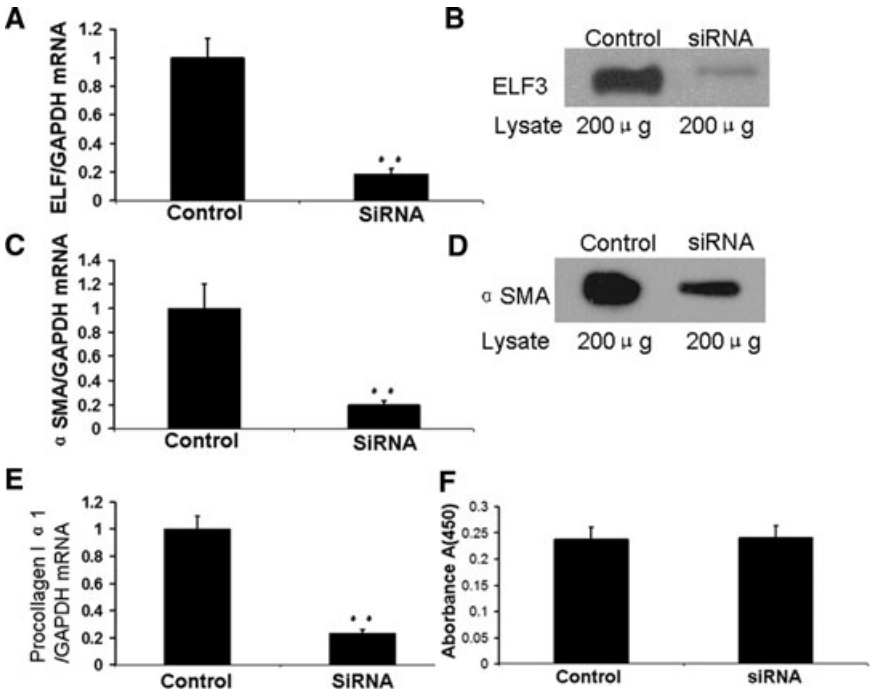

Fig. 2 ELF siRNA-mediated inhibition of HSC activation *in vitro*. (**A**) ELF mRNA was reduced in activated HSCs transfected synthetic siRNA against ELF as assessed by real-time RT-PCR. $P < 0.01$ for ELF siRNA *versus* siRNA control. (**B**) Western blot analysis confirmed that synthetic siRNA inhibited ELF expression in activated HSCs. (**C**) Real-time RT-PCR was used to analyse α-SMA expression in activated HSCs transfected with ELF siRNA. $P < 0.01$ for ELF siRNA *versus* siRNA control. (**D**) α-SMA expression in protein level was suppressed in activated HSCs transfected with ELF siRNA. (**E**) mRNA transcript of α1 procollagen I, principal component of ECM was inhibited in ELF siRNA-transfected HSCs as assessed by quantitative real-time PCR. $P < 0.01$ for ELF siRNA *versus* siRNA control. (**F**) HSC proliferation was evaluated by BrdU incorporation.

bridging fibrosis, decreased in the regeneration of hepatocyte nodule (Fig. 1C). Quantitative RT-PCR (Fig. 1D) confirmed the reduction of ELF expression in regenerative hepatocytes isolated from cirrhotic liver compared with the control. To determine whether activated HSCs express ELF mainly *in vivo*, liver sections from CCl_4-injured mice were stained with the antibodies against ELF and α-SMA. The double immunofluorescence identified overexpression of ELF in activated HSCs (Fig. 1E). ELF becomes highly overexpressed predominantly cytoplasmic and nuclearly in activated HSCs (Fig. 1C). In contrast with ELF expression in normal liver through immunohistochemical staining, immunofluorescence results showed no ELF detection in liver of normal mice (control) because the kit for immunohistochemical staining used was more sensitive.

The effect of siRNA against ELF on characteristic of activated HSCs cultured *in vitro*

Activated HSCs isolated using standard gradient methods more closely resembled activated stellate cells from fibrotic liver, they has been used extensively to model and examine the changes that take place during the phenotype switch of quiescent HSCs to myofibroblasts [11]. First, we found that ELF expression increased significantly in activated HSCs *in vitro* compared with quiescent HSCs (Fig. S3). Then, we delivered synthetic siRNA against ELF into activated HSCs isolated from mice. ELF mRNA and protein were reduced remarkably in activated HSCs transfected with ELF siRNA compared with control siRNA as assessed by quantitative PCR (Fig. 2A) and Western blot (Fig. 2B). Activated HSCs exhibit characteristic of highly proliferative activity, development of prominent bundles of α-SMA filaments and secretion of large amounts of ECM components. Inhibition of ELF expression resulted in a significant reduction in α-SMA expression in activated HSCs *in vitro* as assessed by real-time RT-PCR (Fig. 2C) and Western blot analysis (Fig. 2D). It indicated that ELF was required for HSC activation because α-SMA is a widely accepted marker of activated HSCs. Further study showed a marked inhibition of mRNA transcripts for procollagen (I) in activated HSC transfected with ELF siRNA (Fig. 2E), which revealed that ELF was essential to ECM deposition because collagen I is the principal component of fibrotic scar. To elucidate whether ELF is necessary for HSCs proliferation, proliferative activity of HSCs was evaluated through BrdU incorporation. BrdU assay demonstrated that there was no difference in proliferative activity between activated HSCs treated with ELF-siRNA and siRNA control (Fig. 2F). It indicated that ELF was not necessary for HSC proliferation.

ELF expression in acute liver injury

Mice model of acute liver injury (ALI) was confirmed by alanine aminotransferase, aspartate transaminase (Table S1) and HE (Fig. S5) staining. Quantitative PCR (Fig. 3A) and Western blot (Fig. 3B) demonstrated that similar level of ELF expression was observed in ALI and control mice. Then ELF expression in

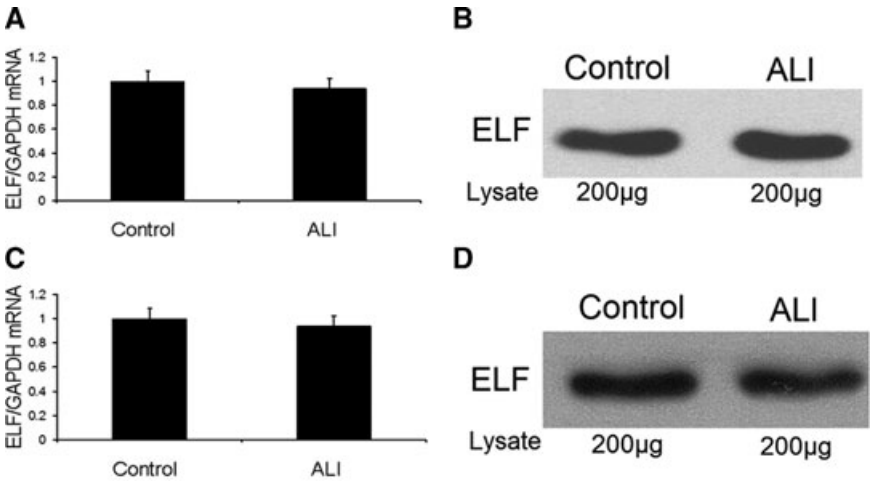

Fig. 3 Hepatic expression of ELF in acute liver injury (ALI). (**A**) Real-time RT-PCR analysis evaluated hepatic ELF expression in normal or ALI mice. No significant difference in ELF mRNA between normal and ALI mice was observed. (**B**) Western blot analysis examined ELF expression in normal or ALI mice. No significant difference in ELF protein between normal and ALI mice was observed. (**C**) Real-time RT-PCR determined ELF expression in hepatocytes isolated from normal or ALI mice. (**D**) Western blot analysis evaluated ELF expression in isolated hepatocytes in control or ALI mice.

hepatocytes isolated from control and ALI mice was determined through real-time RT-PCR and Western blot. The results (Fig. 3C and D) showed there was no difference in ELF expression between normal mice and ALI mice. It indicated that chemical-induced liver damage shown as hepatocellular necrosis and inflammatory infiltration had no effect on ELF expression in hepatocytes.

The relation between HPC expansion and the reduction of ELF expression in regenerative hepatocytes

As described earlier, we demonstrated that hepatic inflammatory reaction and chemical damage did not take any effect on the reduction of ELF expression in CCl_4-treated mice. It indicated that ELF was involved in regeneration of hepatocytes nodule in cirrhotic liver. Immunostaining of CK19, a HPC marker revealed that a dramatic expansion of CK19-positive cell in cirrhotic mice compared with normal and ALI mice (Fig. 4A), which indicated that HPC contributed to regeneration of hepatocytes nodules in cirrhotic liver. To determine the ability of mature hepatocytes to proliferate in cirrhotic liver, we performed Ki67 staining of liver sections from mice receiving CCl_4 treatment. We saw a rapid burst in Ki67-positive hepatocytes in mice receiving CCl_4 treatment at day 7, which revealed the proliferation of mature hepatocytes. Later, it decreased significantly as a result of the loss of mature hepatocytes proliferation upon repeated liver injury, and then increased remarkably from day 56, which revealed HPC proliferation (Fig. 4B). All these demonstrated that regenerative nodules of hepatocytes were derived from HPC expansion. To confirm the relation between HPC expansion and the reduction of ELF expression in regenerative hepatocytes, we performed the timeline-based study on hepatic expression of CK19 and ELF in CCl_4-treated mice. After day 7, HPC activation assessed by CK19 staining was observed in damaged liver, either isolated or forming small clusters consisting of two to three cells; from day 14, CK19-positive cells were more numerous, forming clusters that contained an increasing number of cells (Fig. 4C and E). Although ELF expression in isolated hepatocytes from CCl_4-treated mice decreased remarkably at day 28 (Fig. 4D and F). Thereafter, the reduction of ELF in regenerative hepatocytes over time was consistent with HPC expansion. All these indicated that activation of HPC occurred as an initial phase, before the reduction of ELF expression in regenerative hepatocytes, which was derived from HPC differentiation.

Increased proliferative activity in regenerative hepatocytes of cirrhotic liver

As shown in Figure 5A and B, increased PCNA expression was observed in all hepatic zone containing periportal region and regenerative hepatocyte. It indicated that regenerative hepatocytes possessed increased proliferative activity compared with the control. Then we examined the expression of CDK4, cyclin D1 and pRb. Western blot results showed the expression of CDK4, cyclin D1 and pRb increased in isolated regenerative hepatocytes with the reduction of ELF, assuming in alternation of G1/S checkpoint regulation (Fig. 5B). These results suggested that the loss of ELF in regenerative hepatocytes led to cell-cycle deregulation by alternation of G1/S checkpoint.

We transduced ELF siRNA into AML-12 cell, a murine immortalized hepatocytes [24], and assessed AML-12 proliferation through BrdU incorporation. AML-12 showed increased proliferative response after efficient siRNA treatment (Fig. 5C). It suggested that ELF regulated hepatocyte growth through inhibiting hepatocyte proliferation. It was consistent with previous studies that demonstrated TGF-β-induced growth inhibition and apoptosis in hepatocytes [23, 25, 26].

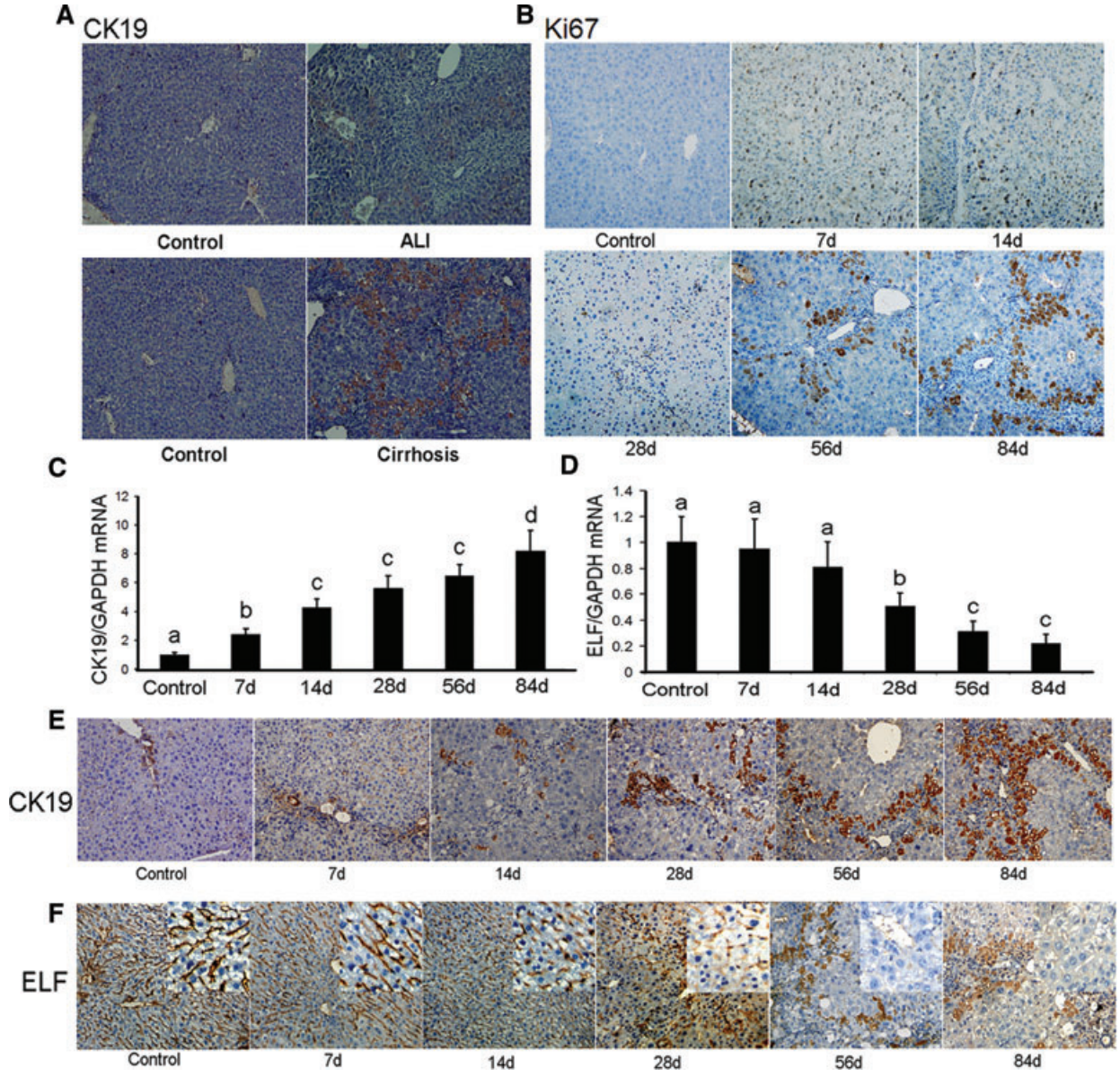

Fig. 4 The relation between HPC expansion and the reduction of ELF expression in regenerative hepatocytes. (**A**) Immunohistochemistry was used to analyse expression of CK19, a marker of HPC in control liver, acute injured and cirrhotic liver. CK19 increased significantly in cirrhotic liver, which revealed that HPCs were activated upon repeated hepatic damage. We also found weak CK19-postive cells scattered in acute injured liver. Magnification 100×. (**B**) Ki67 staining of liver sections from mice receiving CCl_4 treatment for 0, 7, 14, 28, 56 and 84 days. Ki67-positive hepatocytes were observed in mice receiving treatment at day 7 and 14, which revealed the proliferation of mature hepatocytes. Fewer Ki67-positive hepatocytes were present at day 28 because of damaged proliferative capacity of hepatocytes upon repeated liver injury. Ki67-positive cells increased remarkably from day 56. They distributed along the fibrous septa, which revealed the proliferation of HPC. Magnification 200×. (**C**) Quantitative RT-PCR analysis evaluated hepatic CK19 expression in mice receiving CCl_4 treatment for 0, 7, 14, 28, 56 and 84 days. Compared with controls, CK19 mRNA increased 2.6 times after 7 days of CCl_4 treatment and then gradually rose to reach more than six times higher than in controls. (**D**) ELF expression in hepatocytes isolated from CCl_4-induced liver injured model of mice was determined *via* quantitative RT-PCR at different time. ELF expression reduced conspicuously from day 28, and to 23% of control level at day 84. (**E**) HPC activation was evaluated in mice receiving CCl_4 treatment *via* CK19 staining. In livers section obtained from mice receiving CCl_4 treatment, CK19-positive cells increased in number from day 7, formed cluster in the periportal areas and areas of bridging fibrosis with the development of liver fibrosis. CK19-positive cells were restricted to bile ducts in the liver of control mice. Magnification 200×. (**F**) Liver section from mice receiving CCl_4 treatment was stained with ELF antibody. The reduction of ELF expression in mice liver was found remarkably from day 28. Magnification 200×. Note: Data identified by a different letter (a, b, c, d) were significantly different.

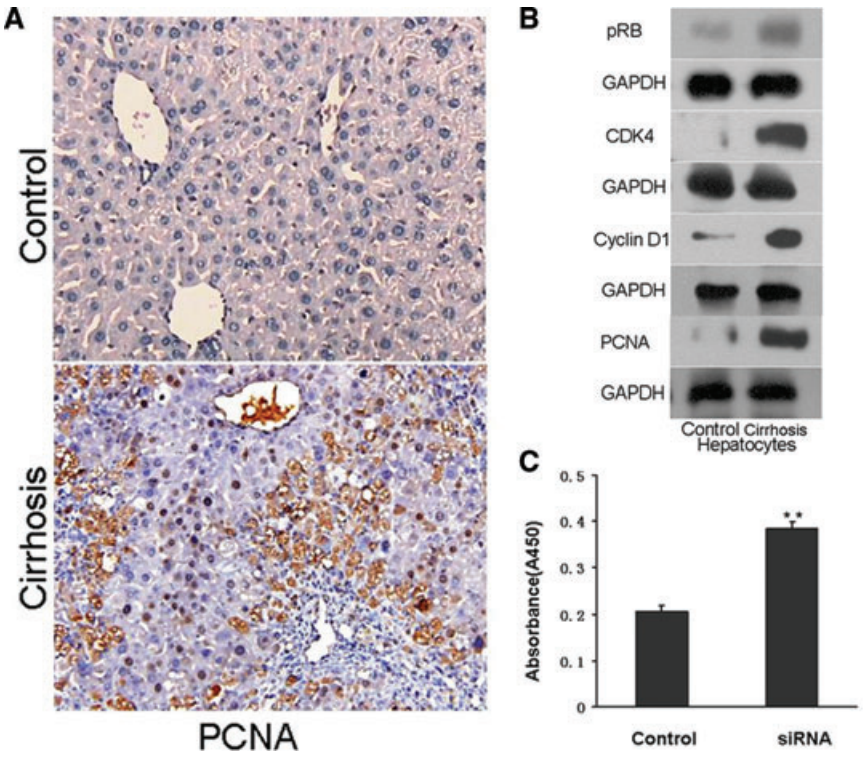

Fig. 5 The proliferation of regenerative hepatocytes in cirrhotic liver. (**A**) Liver sections obtained from control and cirrhotic mice were stained with antibody directed against PCNA. Immunohistochemical analysis revealed that PCNA-positive cells distributed in area of cirrhotic nodules and periportal region. Compared with the control, week staining of PCNA-positive cells was observed in the nucleus of regenerative hepatocytes. In cirrhotic liver, quiescent HSCs undergo activation to highly proliferative myofibroblasts. Activated HSCs assessed by staining of α-SMA, a marker of myofibroblast activation distributed mainly in periportal region, which suggested PCNA-positive activated HSCs in periportal region. Magnification 400×. (**B**) Hepatocytes isolated from mice model of liver cirrhosis induced by CCl_4 were harvested, and then we analysed the patterns of cell cycle regulatory protein in isolated hepatocytes by western blot. The induction of pRB, CDK4, cyclin D1, PCNA in regenerative hepatocytes was observed. GAPDH was used as loading control. (**C**) The effect of ELF siRNA on proliferative capacity of AML-12 was evaluated through BrdU assay. Proliferative capacity of AML-12 increased after efficient siRNA transfection. It indicated that ELF inhibits proliferation of hepatocytes.

ELF involved in TGF-β/Smad signal in HSCs and AML-12 cells

Previous studies demonstrated the involvement of ELF in TGF-β signal pathway [7, 8, 27], so the experiments were carried out to determine how ELF participated in TGF-β/Smad signal. First, lysates from cirrhotic liver were subjected to immunoprecipitation and then immunoblot with Smad and ELF antibodies. As shown in Figure 6A, the results clearly revealed that ELF interacted with Smad3 and Smad4. No interaction between ELF and Smad2 was found. In addition, we investigated ELF–Smad3–Smad4 interactions in activated HSCs cultured *in vitro*. As expected, confocal results showed that ELF, Smad3 and Smad4 colocalized mainly in the nucleus in ultrapurified culture-activated HSCs in which TGF-β/Smad signalling pathway was activated. After efficient ELF knockdown by siRNA, ELF expression decreased significantly in nucleus and diffused in the cytoplasm slightly. Simultaneously, confocal results revealed that Smad3 and Smad4 diffused in cytoplasm and nucleus after synthetic siRNA against ELF transduction into activated HSCs cultured *in vitro*. The intensity of Smad3 and Smad4 in nucleus became weaker remarkably (Fig. 6B and C). We also identified the ELF expression in AML-12 cell through immunofluorescence. ELF was localized in cytoplasm, and translocated into the nucleus after TGF-β_1 stimulation (Fig. 6D).

Discussion

Given the findings that TGF-β_1 plays a crucial role in liver fibrosis, we investigated the expression of ELF, an adaptor of TGF-β/Smad signalling in cirrhotic liver. In mice model of liver cirrhosis, up-regulation of ELF expression in activated HSCs and down-regulation of ELF expression in regenerative hepatocytes of cirrhotic nodules were observed. Then we explored the mechanistic role of ELF in pathogenesis of liver cirrhosis; however, it is unsuitable to evaluate ELF function in pathogenesis of liver cirrhosis *in vivo* using non-selective knockout or transgenic mice because of the discrepancy in ELF expression between activated HSCs and regenerative hepatocytes in cirrhotic liver.

First, we investigated the role of ELF in HSC activation. We have demonstrated that ELF contributed to HSCs activation and the production of procollagen I through the effect of ELF siRNA on characteristic of activated HSCs cultured *in vitro*. Genetic studies in TGF-β_1 transgenic, knockout and inducible transgenic mice showed that TGF-β_1 was responsible for up-regulation of ECM proteins and acceleration of HSC activation [12–15]. BrdU assay showed that the reduction of ELF expression did not inhibit proliferation of activated HSCs cultured *in vitro*, which indicated that ELF was not essential to HSCs proliferation. Of cytokines involved in fibrogenesis, platelet-derived growth factor is the most potent

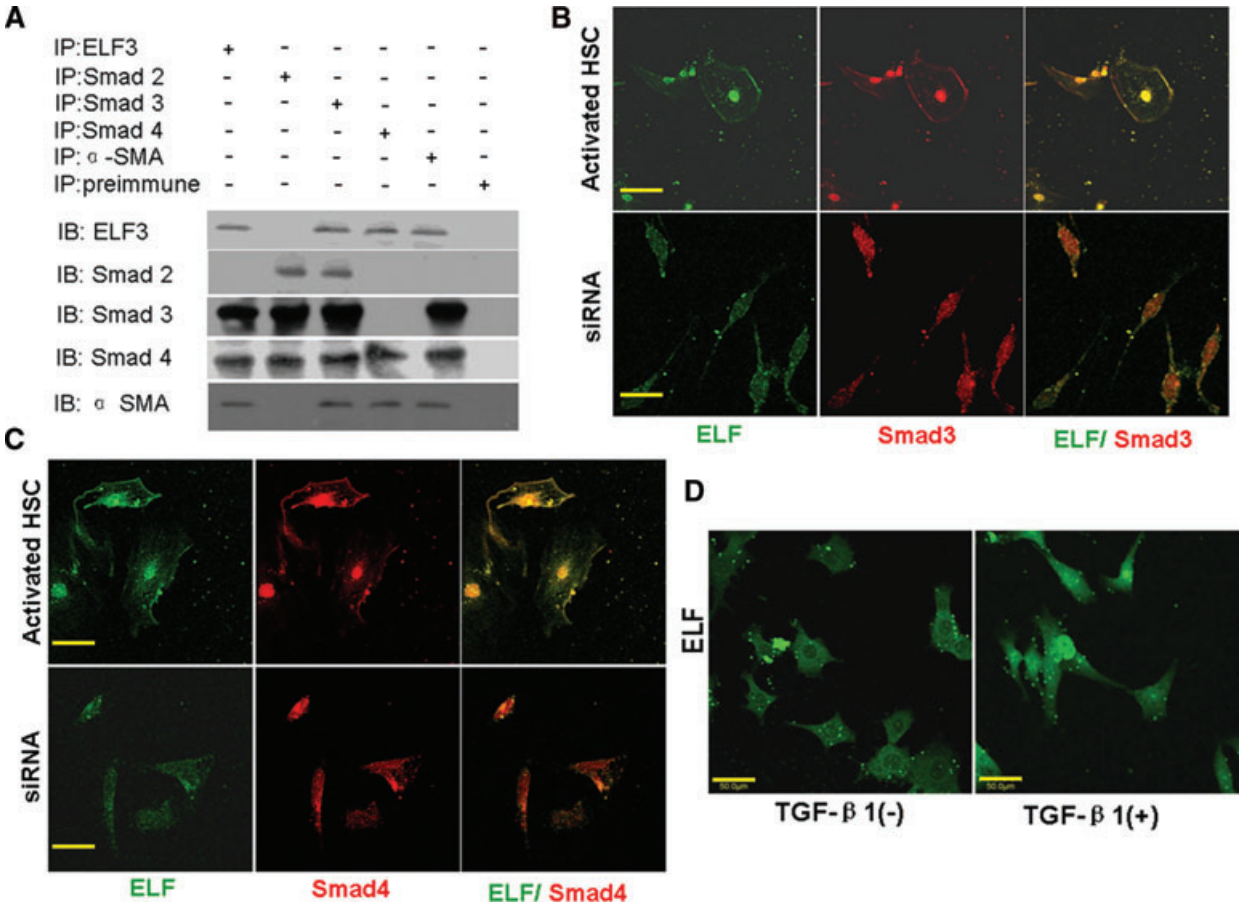

Fig. 6 The role of ELF involved in TGF-β/Smad signal pathway in activated HSCs and hepatocytes *in vitro*. (**A**) Lysates from cirrhotic liver was subjected to immunoprecipitation with preimmune sera, antibody to ELF or Smad; and followed by immunoblotted (IB) with ELF or Smad protein. Coprecipitation of Smad3-ELF, Smad4-ELF was demonstrated. (**B**) Subcellular colocalization of ELF and Smad3 in activated HSCscultured *in vitro*. ELF and Smad3 were present predominantly in the nucleus, independent of TGF-β_1 stimulation. It indicated that TGF-β/Smad signal pathway was activated in activated HSCs *in vitro*. Confocal microscope showed that colocalization of ELF and Smad3 in the nucleus of activated HSCs. Smad3 was reduced in nucleus and diffused in cytoplasm after siRNA knockdown of ELF. It indicated that Smad3 mislocalization because of the loss of ELF. Scale bars, 50 μm. (**C**) Subcellular colocalization of ELF and Smad4 in activated HSCs cultured *in vitro*. Confocal results showed the same pattern of Smad4 expression as Smad3 in activated HSCs and siRNA-treated HSCs. Scale bars, 50 μm. (**D**) Immunofluorescence for ELF in AML12 cells in the absence (control) or presence of 5 ng/ml TGF-β_1 for 6 hrs was examined. The result showed ELF nuclear translocation in AML-12 cell after TGF-β treatment. Scale bars, 50 μm.

proliferative stimulus towards stellate cells. It revealed that HSC proliferation may not dependent on TGF-β/Smad signal. Alternatively, ELF may exerts its effect through TGF-β/Smad-independent pathways. This finding suggested that ELF played a critical role in liver fibrosis, thereby revealing a reduction in ELF expression in activated HSCs may lead to the development of potential antifibrotic therapies. Effective targeted delivery of drugs into activated HSCs *in vivo* enhanced their efficacy and diminished potential side effects. Available strategies for HSC-specific targeting included specific receptors which contained mannose-6-phosphate for uptake *via* the insulin-like growth factor II receptor [28, 29], peptides that recognize the collagen type VI [30] or platelet-derived growth factor receptors [31] and vitamin A-modified liposomes that were taken up by HSCs *via* the RBP receptor [32]. Specific promoter such as SMA promoter also delivered target gene into activated HSCs [33]. Confocal results showed the mislocalization of Smad3 and 4 in activated HSCs tranfected with ELF siRNA. Therefore, it is conceivable that ELF interacts with Smad3/4 in the cytoplasm, and assists in transporting the complexes into the nucleus.

Interestingly, we found the reduction of ELF expression in regenerative hepatocytes of cirrhotic nodule. Mice model of ALI demonstrated that hepatocellular necrosis and inflammatory infiltration did not have any effect on ELF expression in hepatocytes.

Growing evidence [34–38] and our results confirmed that HPC in the periportal canals of Hering was the main resource of regenerative hepatocytes because proliferative capacity of mature hepatocytes was damaged in cirrhotic liver upon repeated chronic injury. Further study indicated that HPC activation occurred before the reduction of ELF expression in regenerative hepatocytes. So it indicated that reduction of ELF expression was involved in the formation of regenerative nodule derived from HPC in pathogenesis of liver cirrhosis. TGF-β family proteins are thought to play a role in the maintenance and differentiation of somatic stem cells, particularly of the gastrointestinal tract [39–41]. Ample evidence revealed that disruption of TGF-β signalling contributed to impaired differentiation of stem cell and allowed for the development of cancers [3, 4, 42]. Recent studies convinced that disruption in TGF-β signalling mediated by loss of ELF contributed to the progression towards carcinogenesis [27, 43, 44]. Genetic studies in mice found that 40–70% of $elf^{+/-}$ mice spontaneously develop hepatocellular cancer [27, 45], Tang *et al*. demonstrated that deregulation of TGF-β signalling mediated by loss of ELF contributed to the transformation of a normal hepatic stem cell to a cancer stem cell, which provided the link between the differentiation of stem cells and carcinogenesis [45]. These indicated that ELF appeared to be a key mediator in HPC differentiation. The reduction of ELF expression in regenerative hepatocytes may be associated with differentiation of HPC into regeneration nodule of hepatocytes. Deregulation of the cell cycle has been recognized as an important factor in tumourigenesis. In cancer cells, aberrant expression of cyclins and CDKs resulted in deregulated cellular growth, which was involved in oncogenic transformation. Cell cycle deregulation and loss of stem cell phenotype were observed in TGF-β adaptor $elf^{-/-}$ mouse brain [43]. Hepatocytes in cirrhotic liver showed weak staining of PCNA, which indicated that regenerative hepatocytes possessed increased proliferative capacity compared with the normal control. Then we examined expression pattern of critical regulators of the G1/S transition in normal hepatocytes and regenerative hepatocytes of cirrhotic nodule. Our study showed elevate level of CDK4, cyclinD1 and phosphorylation of Rb was detected in regenerative hepatocytes isolated from cirrhotic liver, which suggested the deregulation of cell cycle in regenerative hepatocytes with reduction of ELF expression. Hepatocytes in $elf^{+/-}$ mice showed abnormal growth of the cells resulting in dysplasia having large irregular nuclei with clear cytoplasmic enlargement [7]. Liver cirrhosis initiated by chronic hepatitis, extensive alcohol intake or toxins may progress to adenoma and dysplastic nodule formation, develop HCC eventually. Tang *et al*. [45] and we (Fig. S6) found that ELF decreased significantly in HCC compared with normal liver tissue and regenerative nodule of hepatocytes in cirrhotic liver. So it indicated the reduction of ELF expression provided a link between cirrhosis and hepatocellular cancer as a directed consequence of dysregulated differentiation of HPC. The abnormalities of TGF-β signalling mediated by loss of ELF results in deregulated differentiation of HPC, which is considered a crucial step in the development of tumour formation. HPC activation following repeated injury may be more prone to dysplasia, and subsequent malignant transformation when the loss of TGF-β signalling occurs. However, the precise mechanisms by which ELF regulates the differentiation of HPC should be investigated in future.

Acknowledgements

The authors thank Scott L. Friedman (Mount Sinai Medical College) and David A. Brenner (University of California, San Diego, School of Medicine) for assistance with HSC isolation, and Jianguo Song (Shanghai Institutes for Biological Sciences, Chinese Academy of Sciences) for providing AML-12 cell. This study was supported by grants from National Natural Science Foundation of China (30600277 and 81072003).

Conflict of interest

No conflicts of interest were declared.

Supporting information

Additional Supporting Information may be found in the online version of this article:

Fig. S1 Collagen deposition in cirrhotic liver was evaluated by sirius red staining.

Fig. S2 Expression of SMA was determined by immunohistochemical analysis.

Fig. S3 ELF expression in quiescent and activated HSCs.

Fig. S4 Primary hepatocytes were isolated from mice, and then immunostained with albumin, a marker of hepatocytes.

Fig. S5 Liver sections from acute liver injury and normal mouse were examined by haematoxylin–eosin (HE) staining.

Fig. S6 Down-regulation of ELF expression in HCC.

Table S1 ALT and AST values in normal and ALI (acute liver injury) mice

Please note: Wiley-Blackwell is not responsible for the content or functionality of any supporting information supplied by the authors. Any queries (other than missing material) should be directed to the corresponding author for the article.

References

1. **Derynck R, Zhang Y, Feng XH.** Smads: transcriptional activators of TGF-beta responses. *Cell*. 1998; 95: 737–40.
2. **Attisano L, Wrana JL.** Signal transduction by the TGF-beta superfamily. *Science*. 2002; 296: 1646–7.
3. **Mishra L, Shetty K, Tang Y, *et al*.** The role of TGF-beta and Wnt signaling in gastrointestinal stem cells and cancer. *Oncogene*. 2005; 24: 5775–89.
4. **Mishra L, Banker T, Murray J, *et al*.** Liver stem cells and hepatocellular carcinoma. *Hepatology*. 2009; 49: 318–29.
5. **Beck KA, Nelson WJ.** The spectrin-based membrane skeleton as a membrane protein-sorting machine. *Am J Physiol*. 1996; 270: C1263–70.
6. **Viel A.** Alpha-actinin and spectrin structures: an unfolding family story. *FEBS Lett*. 1999; 460: 391–4.
7. **Mishra B, Tang Y, Katuri V, *et al*.** Loss of cooperative function of transforming growth factor-beta signaling proteins, smad3 with embryonic liver fodrin, a beta-spectrin, in primary biliary cirrhosis. *Liver Int*. 2004; 24: 637–45.
8. **Tang Y, Katuri V, Dillner A, *et al*.** Disruption of transforming growth factor-beta signaling in ELF beta-spectrin-deficient mice. *Science*. 2003; 299: 574–7.
9. **Bataller R, Brenner DA.** Liver fibrosis. *J Clin Invest*. 2005; 115: 209–18.
10. **Friedman SL.** Molecular regulation of hepatic fibrosis, an integrated cellular response to tissue injury. *J Biol Chem*. 2000; 275: 2247–50.
11. **Friedman SL.** Mechanisms of hepatic fibrogenesis. *Gastroenterology*. 2008; 134: 1655–69.
12. **Hellerbrand C, Stefanovic B, Giordano F, *et al*.** The role of TGFbeta1 in initiating hepatic stellate cell activation *in vivo*. *J Hepatol*. 1999; 30: 77–87.
13. **Kanzler S, Lohse AW, Keil A, *et al*.** TGF-beta1 in liver fibrosis: an inducible transgenic mouse model to study liver fibrogenesis. *Am J Physiol*. 1999; 276 : G1059–68.
14. **Sanderson N, Factor V, Nagy P, *et al*.** Hepatic expression of mature transforming growth factor beta 1 in transgenic mice results in multiple tissue lesions. *Proc Natl Acad Sci USA*. 1995; 92: 2572–6.
15. **Ueberham E, Low R, Ueberham U, *et al*.** Conditional tetracycline-regulated expression of TGF-beta1 in liver of transgenic mice leads to reversible intermediary fibrosis. *Hepatology*. 2003; 37: 1067–78.
16. **Nakamura T, Sakata R, Ueno T, *et al*.** Inhibition of transforming growth factor beta prevents progression of liver fibrosis and enhances hepatocyte regeneration in dimethylnitrosamine-treated rats. *Hepatology*. 2000; 32: 247–55.
17. **Qi Z, Atsuchi N, Ooshima A, *et al*.** Blockade of type beta transforming growth factor signaling prevents liver fibrosis and dysfunction in the rat. *Proc Natl Acad Sci USA*. 1999; 96: 2345–9.
18. **Arias M, Lahme B, Van de Leur E, *et al*.** Adenoviral delivery of an antisense RNA complementary to the 3' coding sequence of transforming growth factor-beta1 inhibits fibrogenic activities of hepatic stellate cells. *Cell Growth Differ*. 2002; 13: 265–73.
19. **Song YH, Chen XL, Kong XJ, *et al*.** Ribozymes against TGFbeta1 reverse character of activated hepatic stellate cells *in vitro* and inhibit liver fibrosis in rats. *J Gene Med*. 2005; 7: 965–76.
20. **Mishra L, Cai T, Yu P, *et al*.** Elf3 encodes a novel 200-kD beta-spectrin: role in liver development. *Oncogene*. 1999; 18: 353–64.
21. **Radaeva S, Wang L, Radaev S, *et al*.** Retinoic acid signaling sensitizes hepatic stellate cells to NK cell killing *via* upregulation of NK cell activating ligand RAE1. *Am J Physiol Gastrointest Liver Physiol*. 2007; 293: G809–16.
22. **Kaimori A, Potter J, Kaimori JY, *et al*.** Transforming growth factor-beta1 induces an epithelial-to-mesenchymal transition state in mouse hepatocytes *in vitro*. *J Biol Chem*. 2007; 282: 22089–101.
23. **Nguyen LN, Furuya MH, Wolfraim LA, *et al*.** Transforming growth factor-beta differentially regulates oval cell and hepatocyte proliferation. *Hepatology*. 2007; 45: 31–41.
24. **Wu JC, Merlino G, Fausto N.** Establishment and characterization of differentiated, nontransformed hepatocyte cell lines derived from mice transgenic for transforming growth factor alpha. *Proc Natl Acad Sci USA*. 1994; 91: 674–8.
25. **Romero-Gallo J, Sozmen EG, Chytil A, *et al*.** Inactivation of TGF-beta signaling in hepatocytes results in an increased proliferative response after partial hepatectomy. *Oncogene*. 2005; 24: 3028–41.
26. **Sanchez A, Alvarez AM, Benito M, *et al*.** Apoptosis induced by transforming growth factor-beta in fetal hepatocyte primary cultures: involvement of reactive oxygen intermediates. *J Biol Chem*. 1996; 271: 7416–22.
27. **Kitisin K, Ganesan N, Tang Y, *et al*.** Disruption of transforming growth factor-beta signaling through beta-spectrin ELF leads to hepatocellular cancer through cyclin D1 activation. *Oncogene*. 2007; 26: 7103–10.
28. **Moreno M, Gonzalo T, Kok RJ, *et al*.** Reduction of advanced liver fibrosis by short-term targeted delivery of an angiotensin receptor blocker to hepatic stellate cells in rats. *Hepatology*. 2010; 51: 942–52.
29. **Beljaars L, Molema G, Weert B, *et al*.** Albumin modified with mannose 6-phosphate: a potential carrier for selective delivery of antifibrotic drugs to rat and human hepatic stellate cells. *Hepatology*. 1999; 29: 1486–93.
30. **Beljaars L, Molema G, Schuppan D, *et al*.** Successful targeting to rat hepatic stellate cells using albumin modified with cyclic peptides that recognize the collagen type VI receptor. *J Biol Chem*. 2000; 275: 12743–51.
31. **Pinzani M, Milani S, Herbst H, *et al*.** Expression of platelet-derived growth factor and its receptors in normal human liver and during active hepatic fibrogenesis. *Am J Pathol*. 1996; 148: 785–800.
32. **Sato Y, Murase K, Kato J, *et al*.** Resolution of liver cirrhosis using vitamin A-coupled liposomes to deliver siRNA against a collagen-specific chaperone. *Nat Biotechnol*. 2008; 26: 431–42.
33. **Son G, Hines IN, Lindquist J, *et al*.** Inhibition of phosphatidylinositol 3-kinase signaling in hepatic stellate cells blocks the progression of hepatic fibrosis. *Hepatology*. 2009; 50: 1512–23.
34. **Falkowski O, An HJ, Ianus IA, *et al*.** Regeneration of hepatocyte 'buds' in cirrhosis from intrabiliary stem cells. *J Hepatol*. 2003; 39: 357–64.
35. **Sun YL, Yin SY, Xie HY, *et al*.** Stem-like cells in hepatitis B virus-associated cirrhotic livers and adjacent tissue to hepatocellular carcinomas possess the capacity of tumorigenicity. *J Gastroenterol Hepatol*. 2008; 23: 1280–6.

36. **Van Hul NK, Abarca-Quinones J, Sempoux C, *et al*.** Relation between liver progenitor cell expansion and extracellular matrix deposition in a CDE-induced murine model of chronic liver injury. *Hepatology*. 2009; 49: 1625–35.
37. **Xiao JC, Jin XL, Ruck P, *et al*.** Hepatic progenitor cells in human liver cirrhosis: immunohistochemical, electron microscopic and immunofluorencence confocal microscopic findings. *World J Gastroenterol*. 2004; 10: 1208–11.
38. **Greenbaum LE, Wells RG.** The role of stem cells in liver repair and fibrosis. *Int J Biochem Cell Biol*. 2009; *doi: S1357-2725(09)00321–5*.
39. **He XC, Zhang J, Tong WG, *et al*.** BMP signaling inhibits intestinal stem cell self-renewal through suppression of Wnt-beta-catenin signaling. *Nat Genet*. 2004 ; 36: 1117–21.
40. **Watabe T, Miyazono K.** Roles of TGF-beta family signaling in stem cell renewal and differentiation. *Cell Res*. 2009; 19: 103–15.
41. **Zaret KS.** Genetic programming of liver and pancreas progenitors: lessons for stem-cell differentiation. *Nat Rev Genet*. 2008; 9: 329–40.
42. **Mishra L, Derynck R, Mishra B.** Transforming growth factor-beta signaling in stem cells and cancer. *Science*. 2005; 310: 68–71.
43. **Golestaneh N, Tang Y, Katuri V, *et al*.** Cell cycle deregulation and loss of stem cell phenotype in the subventricular zone of TGF-beta adaptor elf-/- mouse brain. *Brain Res*. 2006; 1108 : 45–53.
44. **Kim SS, Shetty K, Katuri V, *et al*.** TGF-beta signaling pathway inactivation and cell cycle deregulation in the development of gastric cancer: role of the beta-spectrin, ELF. *Biochem Biophys Res Commun*. 2006; 344: 1216–23.
45. **Tang Y, Kitisin K, Jogunoori W, *et al*.** Progenitor/stem cells give rise to liver cancer due to aberrant TGF-beta and IL-6 signaling. *Proc Natl Acad Sci USA*. 2008; 105: 2445–50.